Published online 12 September 2014 *Nucleic Acids Research, 2014, Vol. 42, No. 18* ***11349–11362***
doi: 10.1093/nar/gku813

Global MEF2 target gene analysis in cardiac and skeletal muscle reveals novel regulation of DUSP6 by p38MAPK-MEF2 signaling

Stephanie Wales[1,2,3], Sara Hashemi[1,2,3], Alexandre Blais[4] and John C. McDermott[1,2,3,5,*]

[1]Department of Biology, York University, 4700 Keele Street Toronto, Ontario, M3J 1P3 Canada, [2]Muscle Health Research Centre (MHRC), York University, 4700 Keele Street, Toronto, Ontario, M3J 1P3 Canada, [3]Centre for Research on Biomolecular Interactions (CRBI), 4700 Keele Street, Toronto, Ontario, M3J 1P3 Canada, [4]Ottawa Institute of Systems Biology, University of Ottawa, Health Sciences Campus, 451 Smyth Road, Ottawa, Ontario, K1H 8M5 Canada and [5]Centre for Research in Mass Spectrometry (CRMS), York University, 4700 Keele Street, Toronto, Ontario, M3J 1P3 Canada

Received June 12, 2014; Revised August 23, 2014; Accepted August 28, 2014

ABSTRACT

MEF2 plays a profound role in the regulation of transcription in cardiac and skeletal muscle lineages. To define the overlapping and unique MEF2A genomic targets, we utilized ChIP-exo analysis of cardiomyocytes and skeletal myoblasts. Of the 2783 and 1648 MEF2A binding peaks in skeletal myoblasts and cardiomyocytes, respectively, 294 common binding sites were identified. Genomic targets were compared to differentially expressed genes in RNA-seq analysis of MEF2A depleted myogenic cells, revealing two prominent genetic networks. Genes largely associated with muscle development were down-regulated by loss of MEF2A while up-regulated genes reveal a previously unrecognized function of MEF2A in suppressing growth/proliferative genes. Several up-regulated (*Tprg*, *Mctp2*, *Kitl*, *Prrx1*, *Dusp6*) and down-regulated (*Atp1a2*, *Hspb7*, *Tmem182*, *Sorbs2*, *Lmod3*) MEF2A target genes were chosen for further investigation. Interestingly, siRNA targeting of the MEF2A/D heterodimer revealed a somewhat divergent role in the regulation of *Dusp6*, a MAPK phosphatase, in cardiac and skeletal myogenic lineages. Furthermore, MEF2D functions as a p38MAPK-dependent repressor of *Dusp6* in myoblasts. These data illustrate that MEF2 orchestrates both common and non-overlapping programs of signal-dependent gene expression in skeletal and cardiac muscle lineages.

INTRODUCTION

Myocyte enhancer factor-2 (MEF2) is a member of the MADS-box super family of transcriptional regulatory proteins originally identified in skeletal muscle but are now an established component in the regulation of a diverse number of tissues, including smooth, cardiac and skeletal muscle, neurons and T cells (1–4). In vertebrates there are four MEF2 isoforms (A–D) which bind to the consensus sequence (C/T TA(A/T)$_4$TA G/A) within the promoter/regulatory regions of genes to regulate gene transcription (5,6). The transcriptional activation properties of MEF2 is regulated by a variety of post-translational mechanisms including regulation by MAPKs, such as p38 and ERK5 (7–9), and PKA (10), and also through interaction with class II HDACs which inhibit MEF2-dependent gene activation (11,12).

The transcriptional networks underlying both cardiac and skeletal muscle gene expression require MEF2 during embryonic and fetal development and for post-natal control of gene expression for tissue homeostasis in adulthood (13–16). During embryonic development *Mef2* is expressed in the somite and the presumptive vertebrate heart in successive waves, beginning with *Mef2c* (2). This is followed shortly thereafter by *Mef2a* and *Mef2d*. MEF2A and MEF2C are required at different stages of the life cycle. Global deletion of *Mef2c* is embryonic lethal due to impaired heart morphogenesis (13) while *Mef2a* is necessary for post-natal function since gene targeting results in mitochondrial and contractile defects in the heart (17). *Mef2d* homozygous null mice have no phenotypic abnormalities unless exposed to cardiac stress (18). Due to the impaired development and embryonic lethality associated with *Mef2* null mice, tissue-specific conditional mutant mice have been useful in fully dissecting the role of MEF2 in a plethora of tissues. Interestingly, individual skeletal muscle deletion

*To whom correspondence should be addressed. Tel: +1 416 736 2100; Fax: +1 416 736 5698; Email: jmcderm@yorku.ca

of *Mef2c*, but not *Mef2a* or *Mef2d* impairs proper muscle development in mice (19,20). However, the MEF2 complex collectively has an important role in response to postnatal injury as a compound conditional deletion of *Mef2a, -c* and *-d* results in an inability to repair muscle after myotrauma (16). Additionally, MEF2 has been implicated in pathological heart hypertrophy in the adult by provoking the induction of fetal gene expression which is a hallmark of cardiomyocyte (CM) hypertrophy in the failing heart (15,21,22).

Functionally, cardiac and skeletal muscles share many properties and are similar in their reliance on a highly ordered sarcomeric structure. However, there are also important differences between the two lineages that are subserved by interrelated but also subtly different programs of gene expression. Since MEF2 is expressed in both cell types it represents a useful paradigm for studying common and non-overlapping patterns of gene expression targeted by a transcriptional regulatory complex. A number of very well characterized MEF2 target genes that encode a network of structural proteins in cardiac and skeletal muscle, such as Acta1, cTnT, MCK, MyHC and MyLC, are already known (reviewed in (23)), and various large-scale surveys to identify MEF2 targets has been completed independently in skeletal and cardiac muscle (24–26); however, a detailed global inventory of MEF2 target genes in both tissues has not been done. A systematic comparison would provide a more complete picture of common and non-overlapping programs of MEF2-dependent gene expression. Moreover, an unbiased identification of MEF2 target genes may also reveal other properties of these lineages that are controlled by MEF2-dependent gene expression. It has been reported that MEF2 fulfills divergent roles in other cell types, such as neurons, B cells and T cells regulating processes, such as apoptosis and survival (27–30). Clearly, MEF2 targets a more diverse set of genes than previously thought, warranting an unbiased comparison of genomic targets in skeletal and cardiac muscle.

Thus, the primary goal of this study was to identify a complete set of MEF2 target loci in skeletal and cardiac muscle using chromatin immunoprecipitation (ChIP) coupled with high-throughput sequencing. The methodology used was ChIP-exo which utilizes exonuclease activity to digest unprotected DNA, and thereby provides refined sequencing data with high resolution identification of bound sequences (31). Here, we report ChIP-exo identified global genomic MEF2A target genes in differentiating myoblast (MB) cells and CMs. These studies characterize common and non-overlapping programs of MEF2-dependent gene expression and also reveal previously unanticipated functions of MEF2 in striated muscle.

MATERIALS AND METHODS

Cell culture

C2C12 MBs and COS7 fibroblasts were obtained from American Type Culture Collection (ATCC). Cells were maintained in Growth Media (GM) consisting of Dulbecco's Modified Eagle's Medium (DMEM) with High Glucose and L-Glutamine (Hyclone) supplemented with 10% fetal bovine serum (FBS; HyClone) and 1% Penicillin/Streptomycin (Invitrogen). C2C12 were induced to differentiate in differentiation medium (DM) containing DMEM/High Glucose/L-Glutamine supplemented with 2% Horse Serum (Hyclone) and 1% Penicillin/Streptomycin for the indicated time. Primary neonatal CMs were prepared from 1- to 3-day-old rats using the Neonatal Cardiomyocyte Isolation System (Worthington Biochemical Corp). Briefly, whole hearts were dissociated with trypsin (Promega) and collagenase (Worthington Biochemical Corp). The cells were re-suspended in F12 DMEM (Gibco) supplemented with 10% FBS, 1% Penicillin/Streptomycin and 50 mg/l gentamycin sulfate (Invitrogen). The isolated cells were plated for 60 min at 37°C, allowing differential attachment of non-myocardial cells. CMs were counted and transferred to pre-gelatin coated 60-mm plates. The day after, medium was removed and replaced with fresh medium. All cells were maintained in an humidified, 37°C incubator at 5% CO_2. Pharmacological drug treatments were completed for the indicated times and replenished with fresh medium every 24 h.

Transfections

COS7 were transfected using the calcium phosphate precipitation method. Cells were then harvested 48 h post-transfection. For siRNA experiments in C2C12 Lipofectamine (Invitrogen) was used according to the manufacturer's instructions. Cells were then harvested 24 h later or the media was changed to DM. Neonatal CMs were transiently transfected with siRNA using Lipofectamine RNAiMAX (Invitrogen) according to the manufacturer's instructions.

Plasmids

Expression plasmids for pcDNA3-MEF2D, pCMV-dsRed2, pMT3-p38 and pcDNA3-MKK6ee have been described (10,32). The following reporter constructs were used: pRL-Renilla (Promega) and pGL3Basic-*Dusp6*-Luciferase (1010 bp; (33)).

Antibodies and reagents

Rabbit polyclonal MEF2A antibody has been previously described (34). The following antibodies were purchased from Santa Cruz: actin (sc-1616), dsRed (sc-33354), MEF2A (sc-313X; used in ChIP), donkey anti-goat IgG-horseradish peroxidase (IgG-HRP) (sc-2020), ERK-1 (sc-93). The following antibodies were obtained from Cell Signaling: p38 (9212), phospho-p38 (9211), phospho-ERK1/2 (4370). Myogenin (clone F5D) monoclonal antibody was provided by the Developmental Studies Hybridoma Bank (DSHB). Goat anti-rabbit IgG-HRP (170–6515) and goat anti-mouse IgG-HRP (170–6516) were from Bio-Rad Laboratories. The remaining antibodies are as follows: MEF2D (BD Biosciences, 610775), DUSP6 (Abcam, ab76310), Rabbit IgG (Millipore, 12–370), IRDye 680RD goat anti-rabbit (LiCOR) and IRDye 680RD goat anti-mouse (LiCOR). SB 202474 (Santa Cruz) and SB 203580 (Cell Signaling) was used at a concentration of 5 μM.

siRNA

Knockdown of target genes was done using siRNA obtained from Sigma-Aldrich and are listed in Supplementary Figure S4. In C2C12 siRNA was transfected at the following concentration: *Mef2a* (30 nM), *Mef2d* (70 nM), *Atp1a2*, *Dusp6*, *Hspb7*, *Kitl*, *Lmod3*, *Mctp2*, *Prrx1*, *Sorbs2*, *Tmem182* and *Tprg* at 50 nM. In CMs siRNA were transfected at a final concentration of 200 nM.

Immunoblots

Cells were washed with 1× phosphate buffered saline (PBS) and lysed in NP-40 lysis buffer (50 mM Tris, 150 mM NaCl, 0.5% NP-40, 2 mM ethylenediaminetetraacetic acid (EDTA), 100 mM NaF and 10 mM Na pyrophosphate) containing protease inhibitor cocktail (Sigma-Aldrich), 1 mM phenylmethylsulfonyl fluoride (Sigma-Aldrich) and 1 mM sodium orthovanadate (Bioshop). Protein concentrations were determined by Bradford assay (Bio-Rad). Note that 20 μg of total protein were resolved on 10% sodium dodecyl sulphate-polyacrylamide gel electrophoresis (SDS-PAGE) and then transferred onto Immobilon-FL Polyvinylidene Difluoride (PVDF) membrane (Millipore) for 1 h or overnight. Non-specific binding sites were blocked using 5% milk in PBS or tris buffered saline (TBS) containing 0.05% Tween-20 (TBS-T). Membranes were incubated with primary antibodies overnight at 4°C in 5% milk in PBS or 5% Bovine Serum Albumin (BSA) in TBS-T. HRP-conjugated secondary antibody was added for 1 h at room temperature. Protein was detected with Enhanced Chemiluminescence (ECL) western blotting substrate (Pierce). In CMs, immunoblots were performed as described above except antibodies were incubated with Odyssey Blocking Buffer (LiCOR) and membranes were imaged using the LiCOR Odyssey System.

Luciferase analysis

Cells were washed with 1× PBS and then lysed in Luciferase Lysis Buffer (20 mM Tris pH 7.4 and 0.1% Triton X-100). Lysate was briefly vortexed and centrifuged at maximum speed for 15 min at 4°C. Enzymatic activity was measured in each sample on a luminometer using Luciferase assay substrate (E1501, Promega) or Renilla assay substrate (E2820, Promega). Immunoblots of luciferase extracts contained equal volumes from each triplicate.

ChIP

Methods were carried out as described previously described (35); however, a third Immunoprecipitation (IP) Wash Buffer was added (IP Wash Buffer III; 20 mM Tris pH 8.1, 250 mM LiCl, 1% NP-40, 1% deoxycholate and 1 mM EDTA).

RNA extraction

Total RNA was extracted from cells using the RNeasy Plus Mini kit (Qiagen) and Qiashredder (Qiagen). RNA was converted to cDNA using Superscript III (Invitrogen) according to the manufacturer's instructions.

Quantitative polymerase chain reaction (qPCR)

Note that 2.5 μl gDNA or cDNA was combined with iTaq universal SYBR Green supermix (Bio-Rad) and 500 nM primers in a final volume of 20 μl. cDNA was diluted 1:10 in Nuclease-free water (Ambion) prior to use. Each sample was prepared in triplicate and analyzed using Rotor-Gene Q (Qiagen). Parameters for quantitative reverse transcriptase-PCR (qRT-PCR): 30 s 95°C, [5 s 95°C, 30 s 60°C] × 40 cycles. Parameters for ChIP-qPCR: 5 min 95°C, [5 s 95°C, 15 s 60°C] × 40 cycles. Fold enrichment (ChIP-qPCR) and fold change (qRT-PCR) was quantified using the ΔΔCt method. In cardiomyocytes, ChIP-qPCR data is presented as percent input. Primers used in ChIP-qPCR and qRT-PCR are listed in Supplementary Figures S5 and S6, respectively.

ChIP-exo

Note that 15 × 10^6 C2C12 (48 h DM) and 8 × 10^6 primary rat CMs were prepared for ChIP-exo as follows: Cells were washed with 1× PBS and treated with 37% formaldehyde (Sigma-Aldrich) for 15 min at 37°C. The cell pellet was isolated similar to ChIP-qPCR as previously described (35). DNA was sonicated to ∼250 bp in length. Cross-linked chromatin was sent to Peconic Genomics with 5 μg anti-MEF2A (Santa Cruz) and Rabbit IgG (Millipore). Peconic Genomics completed ChIP-exo as previously described (31) and the resulting samples were sequenced on the Illumina HiSeq 2000 platform. Illumina CASAVA software was used for base calling and sequencing reads were aligned to the mm10 (MBs) or rn5 (CMs) genome assembly using BWA 0.5.9 (36). Raw data were filtered for a quality score of 37 using SAMtools (37), and duplicates were removed using Picard (http://picard.sourceforge.net/). MACS 1.4.2 was used to do peak calling analysis (38). To identify MEF2A target genes in skeletal and cardiac muscle corresponding to peak location, MEF2A enrichment peaks identified in MACS were converted to mm9 using UCSC LiftOver (39).

RNA-seq

C2C12 were transfected with 30 nM of *Mef2a* siRNA-2 or scrambled control and RNA was then isolated at 48 h DM, as described above, in duplicate. A total of 5 μg of purified RNA was delivered to McGill University and Genome Quebec Innovation Centre (MUGQIC) for cDNA library preparation (Illumina TruSeq mRNA sample preparation kit), RNA-sequencing (Illumina HiSeq 2000; 100 bp paired-end reads; 4 samples per lane) and bioinformatic analysis. The bioinformatic pipeline included Illumina CASAVA software, Trimmomatic (40), and TopHat/Bowtie (41). Sequencing reads were aligned to the mm10 genome assembly. HTSeq-count generated raw read counts which were used to identify differentially expressed genes using edgeR (42) and DESeq (43).

RESULTS

ChIP-exo analysis of MEF2A target genes in skeletal and cardiac muscle identifies overlapping regulatory domains with divergent gene function

To identify novel MEF2A target genes in skeletal and cardiac muscle, ChIP-exo was performed in differentiating cultured C2C12 MBs (48 h DM) and primary CMs using a MEF2A-specific antibody or a rabbit IgG control (Figure 1A). C2C12 MBs fuse into multinucleated myotubes when grown in low serum DM. During the initial phase of myogenesis MEF2A and MEF2D expression increases (Supplementary Figure S1); therefore, ChIP-exo was performed at 48 h DM, a time at which MEF2 transcriptional activity has been documented to be high.

Of the 2783 and 1648 MEF2A peaks discovered in MBs and CMs, respectively, 294 common enrichment peaks were identified (Figure 1B; Supplementary Tables S1–S3). Nearby genes were identified using Genomic Regions Enrichment of Annotations Tool (GREAT; (44)) using the 5 + 1 kb basal promoter with 1 Mb extension rule. Based on this analysis it was possible for some MEF2A peaks to be associated with more than one gene. The 294 common MEF2A binding peaks corresponded to 473 putative MEF2A target gene associations in skeletal and cardiac muscle. Region-gene associations of MEF2A peaks were then compared using five different parameters relative to the transcription start site (TSS): proximal promoter (±5 kb), upstream (−5 to −50 kb), downstream (+5 to +50 kb), intergenic (>50 kb from any gene) or no gene association (Figure 1C). The pattern of MEF2A recruitment to different regions of the genome in skeletal and cardiac muscle was relatively similar. Approximately only 7% of MEF2A peaks in both cell types were associated with the proximal promoter while nearly 63% of all MEF2A peaks were found in the intergenic region.

Further analysis using CENTDIST (45) revealed common transcription factor motifs within MEF2A enrichment peaks (P-value < 0.05; Figure 1D). The top two motifs within skeletal and cardiac peaks were MEF2 and AP-1. CREB and BACH motifs were also prevalent in both data sets, however, it is noted that the BACH motif is quite similar to AP-1. Interestingly, AP-1 motifs were also found to be enriched in a genome-wide screen of MyoD binding sites in skeletal muscle (46). E-box motifs were also enriched in skeletal muscle but ranked position 13.

Finally, the functional role of MEF2A target genes was assessed using Gene Ontology (GO) analysis to identify terms enriched in either Biological Processes or Cellular Component annotations determined in GREAT (Figure 1E; Supplementary Tables S1 and S2). Enriched Cellular Component GO terms were similar in skeletal muscle and CMs with annotations such as Contractile Fiber and Myofibril. GO terms associated with Biological Processes was the first analysis that suggested MEF2A had a different role in skeletal and cardiac tissue, targeting genes that affected MAP kinase activity or apoptosis, respectively. Both cell types, however, were associated with actin organization.

RNA-seq analysis of MEF2A depleted MBs reveals multiple MEF2 gene networks in regulating cell processes

To further interrogate the identification of MEF2A target genes, RNA-seq analysis was performed in C2C12 (48 h DM) depleted of MEF2A using siRNA-mediated gene silencing and compared to a scrambled siRNA control (Figure 2A). Efficiency of MEF2A knockdown at this time point was assessed using immunoblotting comparing two independent siRNAs programmed to target MEF2A (Figure 2B). siMEF2A-2 was subsequently used in RNA-seq analysis which resulted in 828 down-regulated and 452 up-regulated genes (edgeR P-value < 0.05; Supplementary Table S4). The functional role of MEF2A was assessed using GO::TermFinder (47) to identify enriched GO Biological Processes, however, the up- and down-regulated genes were assessed separately. Figure 2C shows the top five GO Biological Processes enriched in each group. This segregation revealed two different roles of MEF2A: Not only does loss of MEF2A lead to a down-regulation of muscle function, as has been previously shown, but also results in the unanticipated up-regulation of genes associated with cellular migration and locomotion, a cellular process previously not associated with MEF2 function.

The differentially expressed genes identified in RNA-seq were compared with those enriched in ChIP-exo analysis in MB (Figure 2D). Up- and down-regulated genes were separated and then grouped as either ChIP (−) or ChIP (+). As expected, a number of MEF2A target genes identified in ChIP-exo were also found to be differentially regulated in MEF2A depleted MBs. A total of 190/828 down-regulated genes and 121/452 up-regulated genes were found to be MEF2A targets in ChIP-exo. The location of each MEF2A enrichment peak of these differentially expressed genes was then assessed (Figure 2E). Genes were grouped into four bins based on the location of the MEF2A enrichment peak relative to the TSS: ±5 kb, −5 to −50 kb, +5 to +50 kb and >50 kb. This classification revealed that the majority of MEF2A recruitment to down-regulated genes occurs equally within the ±5 kb, −5 to −50 kb and +5 to +50 kb regions. In contrast, ∼65% of genes that were up-regulated in response to MEF2A knockdown were associated with MEF2A enrichment peaks >50 kb from the TSS. MEF2A recruitment to the proximal promoter (±5 kb) of up-regulated genes was less than 5%.

Functional analysis of MEF2A target genes

To investigate whether MEF2A shared novel target genes in cardiac and skeletal muscle, the differentially expressed genes identified in RNA-seq were grouped in a similar classification to Figure 2D, however, MEF2A target genes in CM were included. Three divisions of differentially expressed genes were established: ChIP (−), ChIP (+) MB and ChIP (+) MB and CM. Only 4% of differentially expressed genes were identified as MEF2A target genes in MB and CM (Figure 3A). This corresponded to 38 down-regulated and 20 up-regulated genes (Supplementary Table S4). From this list, 10 putative MEF2A target genes were selected for further study. The position of MEF2A recruitment relative to the TSS of each gene is shown in Figure 3B. The presence

A

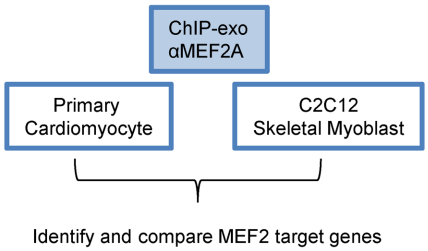

B

C

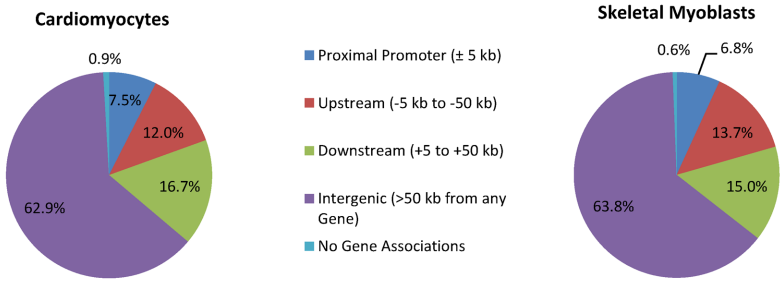

D

Cardiomyocytes

Rank	TF Family	Logo
1	MEF2	
2	AP1	
3	CREB	
4	BACH	
5	ERE	

Skeletal Myoblasts

Rank	TF Family	Logo
1	MEF2	
2	AP1	
3	BACH	
4	CREB	
5	NRF	

E

GO Cellular Component

Cardiomyocytes

Term Name	Binom Raw P-Value
contractile fiber part	5.37899e-17
contractile fiber	6.69078e-17
myofibril	2.02277e-16
sarcomere	3.42137e-15
I band	6.09643e-12

Skeletal Myoblasts

Term Name	Binom Raw P-Value
actin cytoskeleton	8.16180e-21
contractile fiber	3.91908e-14
contractile fiber part	1.01278e-13
myofibril	2.48759e-13
sarcomere	8.10082e-11

GO Biological Processes

Cardiomyocytes

Term Name	Binom Raw P-Value
actin cytoskeleton organization	2.33474e-9
actin filament-based process	4.57545e-9
induction of apoptosis	1.11763e-8
induction of programmed cell death	1.27591e-8
actin filament organization	4.06429e-7

Skeletal Myoblasts

Term Name	Binom Raw P-Value
actin cytoskeleton organization	2.04113e-18
actin filament-based process	2.60016e-18
regulation of MAP kinase activity	7.93509e-17
regulation of protein serine/threonine kinase activity	9.60009e-17
wound healing	3.50272e-12

Figure 1. Identification of MEF2A target genes in MBs and CMs using ChIP-exo. **(A)** Workflow of ChIP-exo analysis. C2C12 (48 h DM; MB) and primary CMs were collected to identify MEF2A target genes using ChIP-exo. A non-specific IgG antibody was used as a control. **(B)** The number of common MEF2A enriched peaks in MB and CM identified in ChIP-exo are indicated in a Venn diagram. **(C)** The percentage of peaks within the proximal promoter (±5 kb), upstream (−5 to −50 kb), downstream (+5 to +50 kb) or intergenic region (>50 kb from any annotated gene) identified in ChIP-exo using GREAT. Location is relative to the TSS. **(D)** The five most dominant transcription factor binding motifs found within MEF2A-enriched peaks as determined by CENTDIST (P-value < 0.05). **(E)** Biological Processes and Cellular Component GO terms of MEF2A enriched peaks from MB and CM.

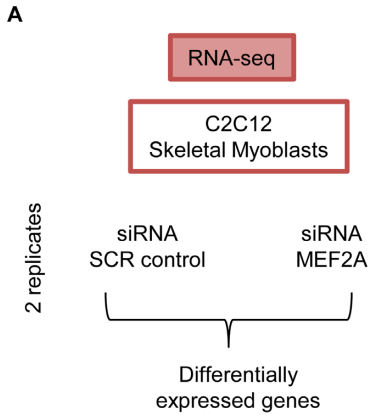

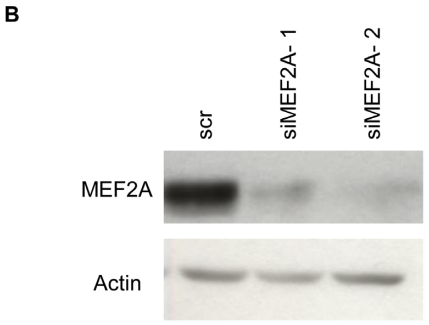

C

GO Biological Processes	*P*-Value
Downregulated (828)	
muscle structure development	4.86E-28
muscle contraction	1.67E-23
muscle system process	7.15E-23
muscle cell differentiation	3.29E-18
muscle organ development	3.26E-17
Upregulated (452)	
regulation of multicellular organismal process	4.15E-15
cellular component movement	2.94E-13
regulation of response to stimulus	1.73E-12
cell migration	2.77E-12
locomotion	2.80E-12

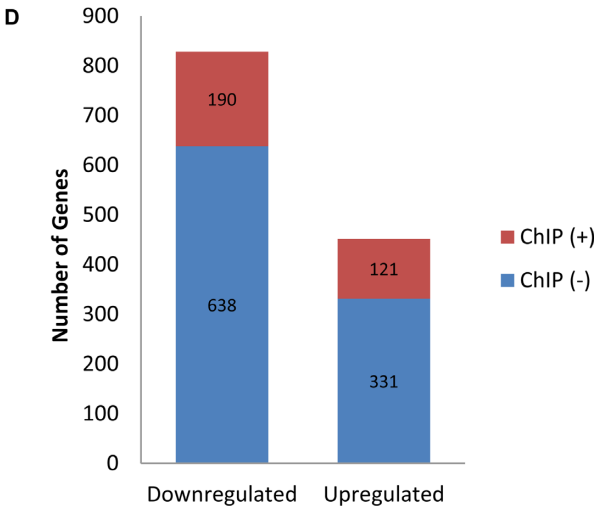

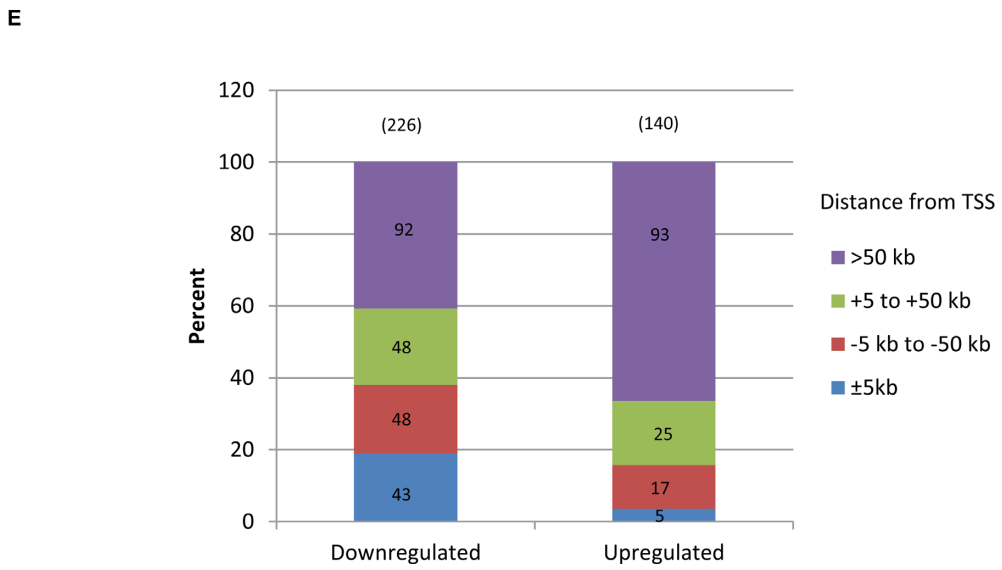

Figure 2. RNA-seq analysis of MEF2A depleted skeletal MBs. **(A)** RNA-seq analysis workflow. MB were transfected with 30 nM of siMEF2A-2 or a scrambled siRNA control. Samples were prepared for RNA-seq analysis in duplicate. Differentially expressed genes were assessed using edgeR *P*-value < 0.05. **(B)** Two different siRNA targeting *Mef2a* were transfected into MBs at 30 nM and allowed to differentiate for 48 h in DM. Cells were harvested and protein was extracted to assess changes in MEF2A using immunoblotting. **(C)** Distinguished roles for MEF2A in skeletal myogenesis were revealed when up- and down-regulated genes were grouped separately prior to GO (Biological Processes) term analysis. **(D)** The differentially expressed genes that were also identified as MEF2A target genes in MB were determined (ChIP (+)). Differentially expressed genes that were not identified as MEF2A targets are labeled ChIP (−). **(E)** Binding profiles of MEF2A recruitment to associated genes in MB based on their differential expression in RNA-seq analysis. The raw gene count is indicated within each section.

A

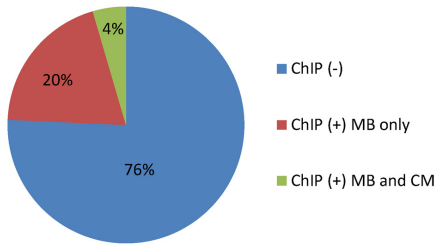

B

Gene Symbol	Distance of MEF2 peak in MB and CM from TSS ±5kb	-5 kb to -50 kb	+5 to +50 kb	>50 kb	MEF2 consensus sequence within 1 kb of peak
Upregulated					
Tprg				·	·
Mctp2				·	
Kitl				·	·
Prrx1				·	
Dusp6	·	·			
Downregulated					
Atp1a2			·		
Hspb7			·		·
Tmem182				·	
Sorbs2				·	
Lmod3	·				·

C

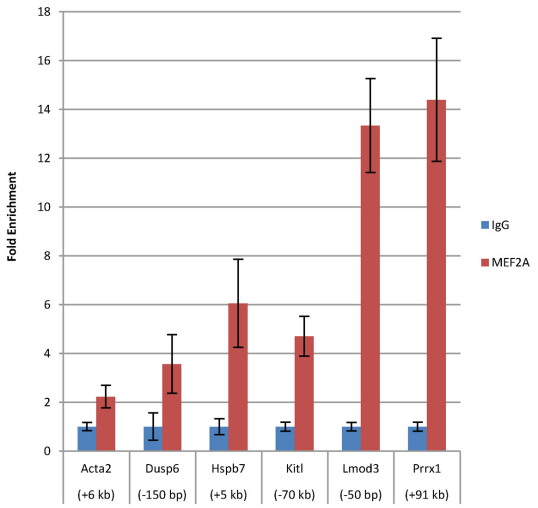

D

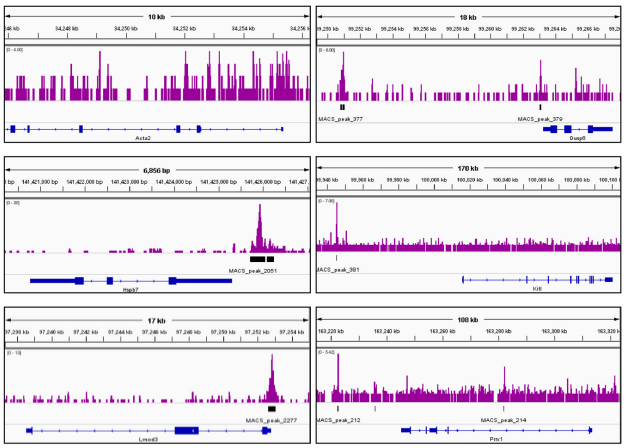

E

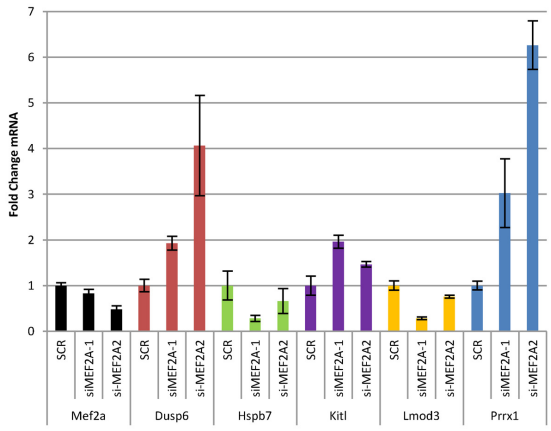

F

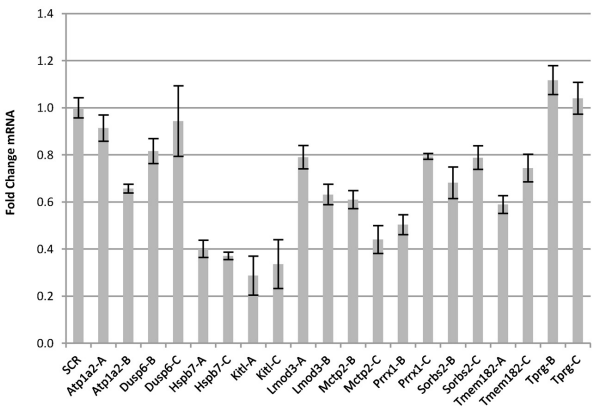

Figure 3. Functional analysis of MEF2A target genes. **(A)** The percentage of differentially expressed genes in MB that were also identified as MEF2A target genes (ChIP (+)) in MB alone or MB and CM. **(B)** Comparative analysis of 10 putative MEF2A target genes. Selected genes were differentially expressed in RNA-seq analysis in MB and shared overlapping MEF2A enrichment peaks in MB and CM. The locations of common MEF2A recruitment peaks relative to the TSS and nearby MEF2 consensus sequences are indicated. **(C)** MEF2A recruitment was assessed in C2C12 (48 h DM) using ChIP-qPCR. *Acta2* was used as a negative control locus. Error bars represent ±SD, $n = 3$. **(D)** Screenshot from IGV depicting C2C12 ChIP-exo read density and MACS peak calls. Read densities are in purple, MACS peak calls are in black and RefSeq genes are in blue. **(E)** Two different siRNA targeting *Mef2a* were transfected into C2C12 at 30 nM and allowed to differentiate for 48 h in DM. Cells were harvested and RNA was extracted to assess changes gene expression using qRT-PCR. Samples were normalized to *β-actin*. Error bars represent ±SD, $n = 3$. **(F)** Knockdown of individual target genes in MB. C2C12 were transfected with 50 nM siRNA and harvested 24 h later. mRNA was assessed similar to that in (E).

of a MEF2 consensus sequence within 1 kb of the enrichment peak is also indicated.

To validate that the identified genes from ChIP-exo and RNA-seq were true MEF2A target genes, *Dusp6* (dual specificity phosphatase 6), *Hspb7* (heat shock protein family, member 7), *Kitl* (kit ligand), *Lmod3* (leiomodin 3) and *Prrx1* (paired related homeobox 1) were chosen for further study. Only *Kitl*, *Lmod3* and *Hspb7* contain nearby MEF2 consensus sequences. We confirmed MEF2A recruitment to these genes using gene targeted ChIP-qPCR in C2C12 at 48 h DM (Figure 3C). Primers were designed to flank the MEF2A enrichment peak or the nearby MEF2 consensus sequence (if present). Figure 3D represents, for each gene, the ChIP-exo sequencing read density in C2C12 as well as MACS peak calls, and was prepared using the Integrative Genome Viewer (IGV; (48)). In some cases, genes had more than one enrichment peak. For example, MEF2A was recruited to two locations upstream of *Dusp6* at ±5 kb and −5 to −50 kb in both CM and MB. In this case, we focused on the more proximal binding event 150 bp upstream from the TSS in ChIP-qPCR analysis. *Prrx1*, however, had three MEF2 binding events in MB but only one (+91 kb; MACS_peak_212) had a common binding event in CM. Using ChIP-qPCR we detected variable MEF2A recruitment at all genes compared to *Acta2*. Interestingly, the level of MEF2A recruitment to target genes in Figure 3C corresponded to similar enrichment patterns detected in ChIP-exo.

Two independent MEF2A siRNAs were individually transfected into MB. At 48 h DM the expression of three up- (*Kitl*, *Prrx1* and *Dusp6*) and two down-regulated (*Hspb7* and *Lmod3*) genes were then assessed (Figure 3E). Similar to RNA-seq results, loss of MEF2A resulted in the down-regulation of *Lmod3* and *Hspb7*. Conversely, *Dusp6*, *Prrx1* and *Kitl* were up-regulated in response to MEF2A knockdown. Interestingly, MEF2D was also shown to be recruited to *Prrx1*, *Lmod3* and *Hspb7* in MBs and these genes were differentially expressed in response to MEF2D overexpression (26).

To begin to understand the functional role of these putative MEF2 target genes we used siRNA gene silencing to suppress the expression of *Atp1a2* (ATPase, Na+/K+ transporting, alpha 2 polypeptide), *Dusp6*, *Hspb7*, *Kitl*, *Lmod3*, *Mctp2* (multiple C2 domains transmembrane 2), *Prrx1*, *Tmem182* (transmembrane protein 182), *Sorbs2* (sorbin and SH3 domain containing 2) and *Tprg* (transformation related protein 63 regulated) and determined their role in myogenesis by assessing changes in *Myogenin* expression in MBs as a readout of the irreversible commitment to myogenic induction (Figure 3F). Prior to this, the efficiency of knockdown of each target gene was determined using three siRNAs labeled A–C (Supplementary Figure S2). The two with the most efficient knockdown of the targeted gene product were selected to assess *Myogenin* expression. The knockdown of a number of these genes resulted in down-regulation of *Myogenin* expression in MBs in GM. In particular, loss of *Hspb7* and *Kitl* reduced *Myogenin* by 50% indicating that a number of the identified MEF2 target genes are crucial for efficient myogenic differentiation and their precise role in the myogenic program remains to be characterized.

DUSP6 is a novel MEF2 target gene in cardiac and skeletal muscle

We were particularly interested in the identification of *Dusp6* as a MEF2A target since it was shown to be necessary in regulating the skeletal muscle satellite cell population and has also been implicated in cardiac hypertrophy (49,50). Based on the overlap of MEF2 recruitment to the *Dusp6* promoter in MBs and CMs and its relative location in relation to other transcriptional regulatory domains of the *Dusp6* gene locus (33), *Dusp6* was selected for further mechanistic analysis in terms of how it is regulated by MEF2.

To confirm that *Dusp6* is also a MEF2A target gene in CMs ChIP-qPCR was done in primary CMs (Figure 4A). This analysis confirmed that MEF2A is recruited to a shared location within the *Dusp6* promoter in both MBs and CMs. Furthermore, MEF2A or MEF2D depletion from CMs (Figure 4B and C) or MBs (Figure 4D) and corresponding DUSP6 expression was assessed in immunoblot analysis. Knockdown of either MEF2 subunit in CMs dramatically increased DUSP6 expression (Figure 4B and C). Although loss of MEF2A at 48 h DM up-regulated *Dusp6* transcription in MBs (Figure 3B), at the protein level, DUSP6 was unaffected by knockdown of MEF2A in C2C12 (24 h DM; Figure 4D) and we suspect this is a temporal lag in response to the knockdown. In contrast, loss of MEF2D (the heterodimeric partner of MEF2A in MBs (51)) increased DUSP6 expression.

Regulation of DUSP6 by MEF2 is p38MAPK-dependent in MBs

DUSP6 is a dual specificity protein phosphatase, predominately targeting ERK1/2 activity (52,53). Interestingly, *Dusp6* expression is mediated by growth factors and ERK1/2 activation in a negative feedback loop (33,54). Upon serum withdrawal in C2C12 MBs we observed a decrease in DUSP6 expression during the initial phase of myogenesis (Figure 5A) under conditions when we have previously documented that MEF2 protein levels and DNA binding activity are increasing (55). In addition, there was a corresponding decrease in ERK1/2 activity and activation of p38MAPK. Since MEF2 becomes activated in part due to phosphorylation by p38MAPK (7) and there is an inverse relationship between DUSP6 expression and p38MAPK activity, we sought to determine whether p38MAPK also has a role in regulating *Dusp6*. C2C12 were treated with a well characterized p38MAPK inhibitor SB 203580 (5 μM) or its inactive analogue SB 202474 as a control. A time course treatment of MBs with or without SB 203580 treatment revealed that while p38MAPK inhibition blocked myogenesis, as shown by a decrease in Myogenin expression, this was accompanied by an up-regulation of DUSP6 (Figure 5B). MEF2A and MEF2D are down-regulated in response to SB 203580 treatment, probably as a result of an overall delay in myogenesis (Supplementary Figure S3). To determine whether p38MAPK was acting directly through MEF2 to modulate DUSP6 expression, C2C12 were transfected with two sets of siRNA targeting *Mef2a* or *Mef2d* and then treated with SB 203580 for 24 h in DM (Figure 5C). p38MAPK inhibitor treatment consistently up-regulated DUSP6, with or without MEF2A. In MEF2D de-

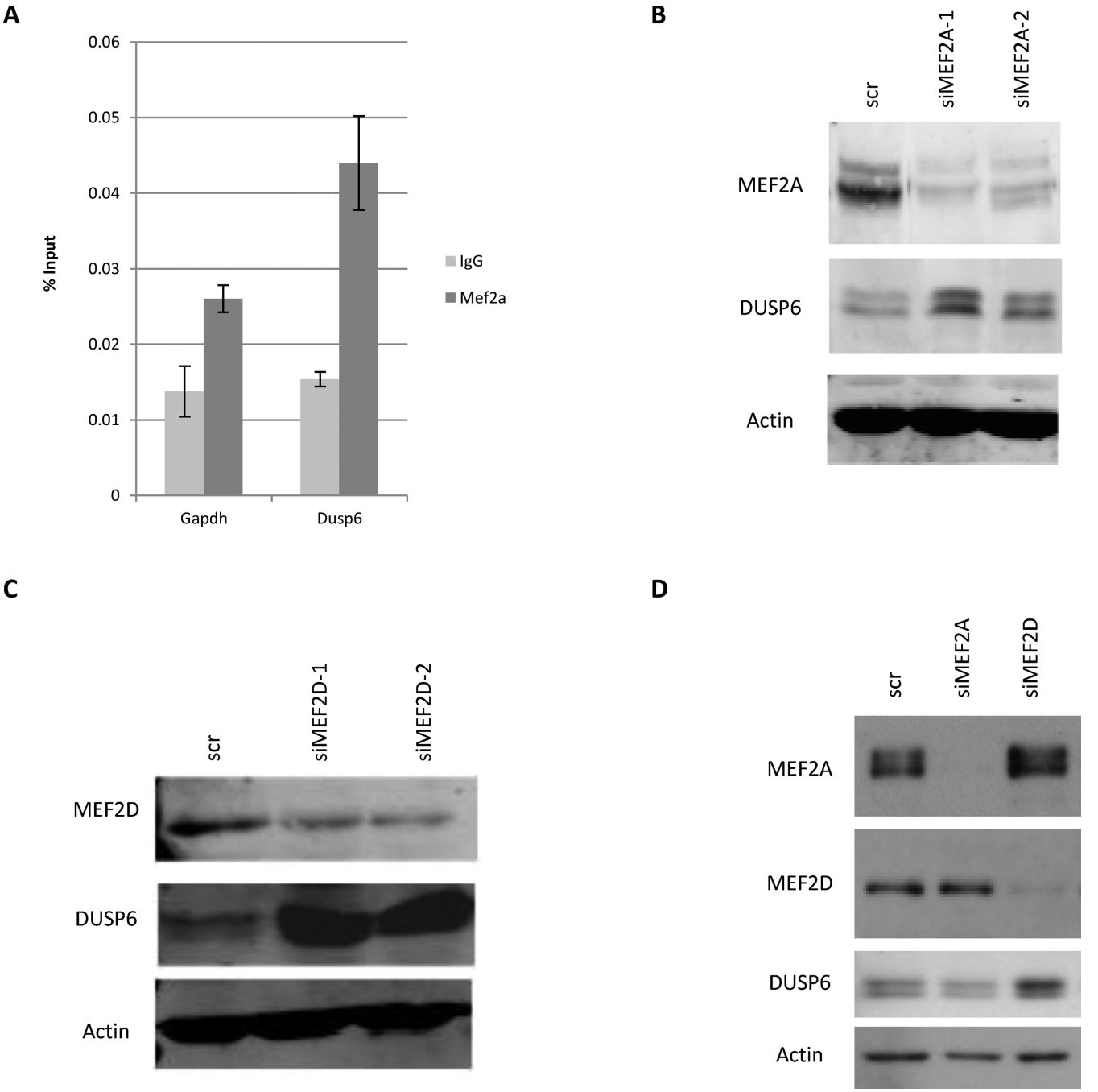

Figure 4. siRNA mediated gene silencing of MEF2 in CMs or MBs induces DUSP6 expression. **(A)** MEF2A is recruited to the *Dusp6* promoter in primary CMs. *Gapdh* was used as a negative control locus. Error bars represent ±SD, $n = 3$. **(B)** Knockdown of MEF2A or MEF2D **(C)** in primary CMs up-regulates Dusp6 expression. siRNA was added at a final concentration of 200 nM. Protein was harvested and analyzed by immunoblotting with the indicated antibodies. **(D)** Knockdown of MEF2D up-regulates DUSP6 expression in MB. *Mef2a* or *Mef2d* were targeted using 30–70 nM siRNA. C2C12 were harvested at 24 h DM for immunoblot analysis.

pleted cells, however, SB 203580 treatment did not have any effect. Our interpretation of these data, in contrast to the usual potentiating effect of p38MAPK on MEF2 activity, is that MEF2D is required for the p38MAPK-dependent repression of DUSP6.

To test this novel observation further in a carefully controlled reconstruction assay we transfected COS cells (as a neutral cell type to circumvent endogenous regulation by factors in MBs) with a *Dusp6* promoter construct, *Dusp6*-luc (1010 bp; (33)), with or without a constitutively active MKK6 (MKK6ee to activate p38MAPK), p38MAPK or MEF2D. The results of this assay were unequivocal in that individually, MEF2D and activated p38MAPK activate expression of the *Dusp6* reporter gene but when transfected in combination, MEF2D and activated p38MAPK cannot induce expression of *Dusp6*-luc (Figure 5D). Also, SB

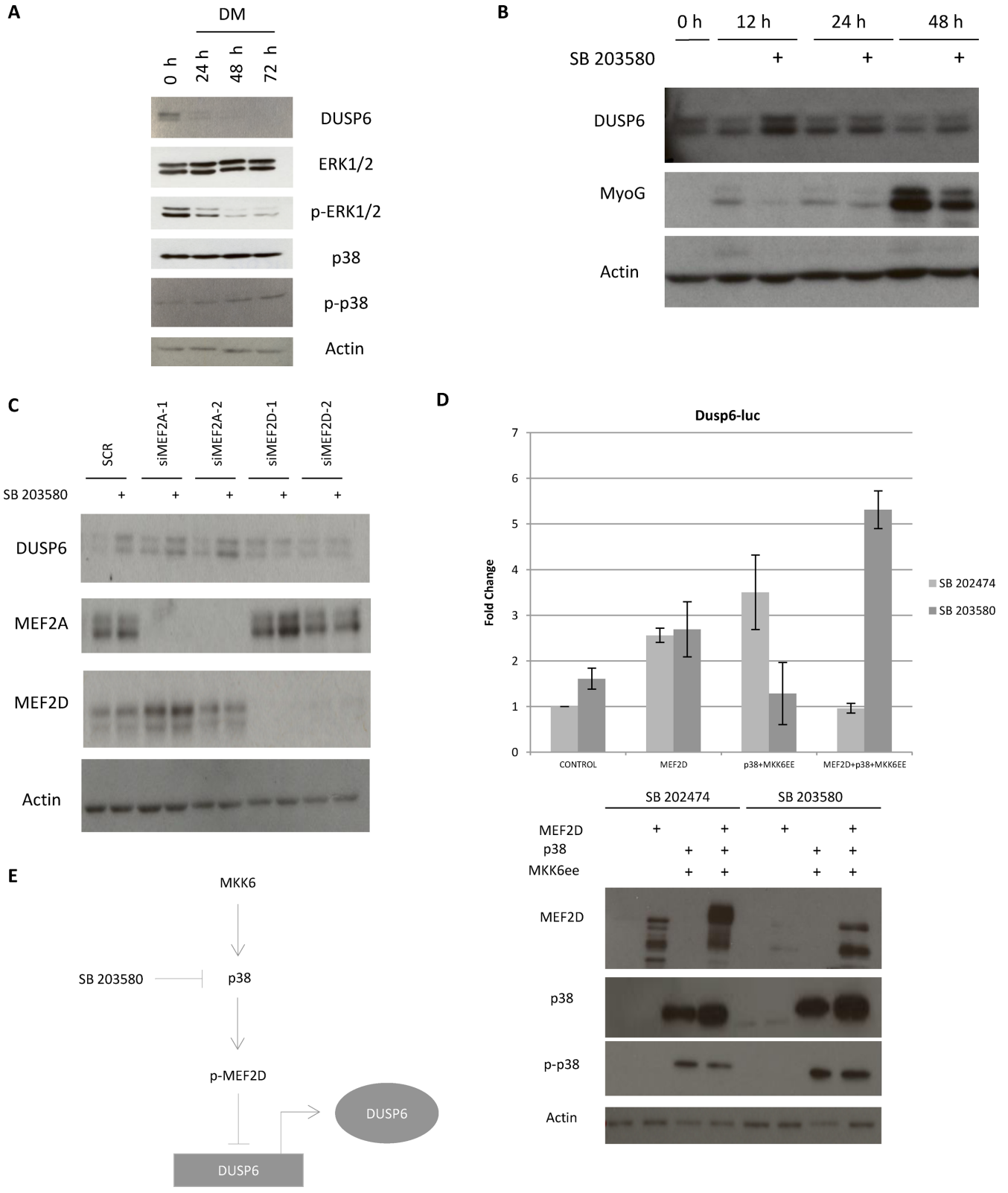

Figure 5. MEF2D inhibits DUSP6 in a p38MAPK-dependent manner in MBs. **(A)** C2C12 were allowed to differentiate, harvested at the times specified and analyzed by immunoblotting with the indicated antibodies. **(B)** Myogenesis is inhibited when C2C12 are treated with p38MAPK inhibitor SB 203580 (5 μM). Media was changed to DM for the indicated time and protein was assessed by immunoblotting. Control cells were treated with an inactive analogue, SB 202474. **(C)** C2C12 were transfected with 30 nM siMEF2A or 70 nM siMEF2D and treated with SB 203580 (5 μM) for 24 h in DM. Cells were harvested as described above. **(D)** COS7 were transfected with *Dusp6*-luc and the indicated plasmids. One day after transfection cells were treated with 5 μM SB 203580 or inactive analogue for 24 h. Luciferase values were normalized to Renilla. Error bars represent ±SEM, $n = 3$. Corresponding immunoblots are shown. **(E)***Dusp6* is negatively regulated by MEF2D in a p38MAPK-dependent manner.

203580 treatment reverses this effect by enhancing *Dusp6* reporter gene activation, further supporting the direct involvement of p38MAPK in this negative regulation. Simultaneous immunoblot analysis of this experiment shows that MKK6ee/p38MAPK induce the previously well characterized post-translational modifications (PTMs) of MEF2 (34) and SB 203580 treatment reverses these PTMs as expected (Figure 5D). Collectively, these data lead us to the novel conclusion that p38MAPK signaling to MEF2D leads to transcriptional repression of the *Dusp6* promoter (Figure 5E).

DISCUSSION

Using forefront methods in genomic analysis we have characterized the panoply of MEF2A genomic targets in striated muscle. Moreover, by coupling this chromatin-based genome-wide analysis of MEF2A DNA binding to MEF2A gene silencing and RNA-seq we have been able to comprehensively catalog both direct and indirect genomic targets of MEF2. These data identify some novel aspects of MEF2 function that have, thus far, not been appreciated. Particularly, this comparative analysis will lead to new directions in understanding the function of MEF2 in a variety of contexts in its role as an important regulator of gene expression in all muscle types, neurons and immune system cells, both during development and in a variety of post-natal physiological and pathological circumstances. In addition, more detailed analysis by gene silencing of some of the identified MEF2A target genes led us to identify a number of downstream targets that fulfill a potentially important role in the myogenic program. Finally, mechanistic studies concerning the regulation of the *Dusp6* locus by MEF2 has led us to the novel conclusion that p38MAPK-MEF2 signaling leads to repression of DUSP6 expression during the myogenic cascade.

ERK1/2 inactivation through DUSP6 expression has been linked to pluripotency in embryonic stem cells (56), cardiac hypertrophy (49,57) and the satellite stem cell pool in muscle (50). Therefore, there is an evident requirement of DUSP6 to down-regulate ERK1/2 signaling in the very early phases of differentiation. In skeletal muscle cells p38MAPK and ERK1/2 exhibit inverse activity: in growth conditions, p38MAPK is inactive and ERK1/2 is active (58), however, upon the withdrawal of growth factors, p38MAPK becomes active, ERK1/2 is inhibited and the myogenic cascade proceeds. The results presented here may be linked to a previously reported biphasic role for ERK1/2 in muscle in which ERK1/2 is implicated in proliferation of MBs under growth conditions but also in differentiation conditions in myotube fusion (59,60). In this model DUSP6 expression itself has to be extinguished for the myogenic program to proceed and for ERK1/2 involvement in MB fusion later in the program. Our contention is, therefore, that the induction of MEF2 and p38MAPK activity at the onset of differentiation is required for the transcriptional suppression of *Dusp6* which then allows myogenesis to proceed.

The canonical interpretation of the p38MAPK-MEF2 signaling pathway has, so far, been that when covalently modified by p38MAPK-mediated phosphorylation, MEF2 transcriptional activation properties are enhanced (7); however, as alluded to above, our data illustrate that MEF2D represses *Dusp6* expression in a p38MAPK-dependent manner. Interestingly, this potently repressive role of MEF2 at some genes may also clarify the previously unexplained observation that in a compound transgenic in which the MEF2 sensor mice were bred with *Mef2a* homozygous nulls, an unexpectedly high β-Galactosidase staining was observed in some tissues in the mice (17). This observation is consistent with a potent repressive effect of MEF2 in certain cellular contexts. Indeed, there have been several negative regulators of MEF2 identified including HDAC4 (11), Cabin1 (61), MITR (62), HIPK2 (63) and PKA (10,64), however, it is unclear at this point how p38MAPK can lead to MEF2-mediated transcriptional repression. Indeed, primary limb mesenchymal cultures treated with p38MAPK inhibitor also exhibited enhanced MEF2 activity which implies that the regulation of MEF2 activity by p38MAPK activity is not as straightforward as previously thought (65).

Dusp6 provides not only an example of a common MEF2 target gene in skeletal and cardiac muscle but also demonstrates the complex role of MEF2 as a heterodimer. Characterization of binding sites of the single *Mef2* gene in *Drosophila* using ChIP-chip and mutagenesis first revealed that MEF2 has a more significant role in muscle development than originally thought and further showed that MEF2 activity is regulated in a complex manner to function differently at certain developmental timepoints (66). In vertebrate development, it is not surprising that with four *Mef2* genes, the complexity of MEF2-dependent gene expression increases. With respect to the role of MEF2A/D heterodimers in skeletal muscle, MEF2A and MEF2D are subject to differential regulation by PKA (10), among other kinases, and MEF2D is differentially spliced in a skeletal muscle-specific manner (26), which together may explain the seemingly more dominant role of MEF2D in regulating *Dusp6* in MB. It is also critical to recognize that the majority of MEF2A target genes identified in CM and MB are not shared. This could be explained by differential upstream signaling, different co-factor interactions, and chromatin accessibility. Although the majority of target genes between CM and MB were different, the predominant transcription factor motifs and GO terms were largely similar indicating conservation of MEF2 function at the level of cellular processes. However, one exception to this is that MEF2A target genes in CM were associated with GO Biological Processes involving apoptosis and cell death. Currently, there is no direct evidence that MEF2 regulates apoptosis in CMs.

In terms of the global target gene network that we have identified, there are some results that surprised us. The first was that some distal MEF2 binding events were observed greater than 50 kb from the TSS. Similar to our findings, MEF2 binds to intra- and intergenic enhancer regions during cardiac hypertrophy (67). Together this indicates that MEF2 has an emerging role as a transcription factor that is able to regulate gene expression globally. Furthermore, MEF2A was recruited to different genomic regions in up- and down-regulated genes. An interesting possibility would be that the position of MEF2 recruitment relative to the TSS dictates its function as a positive or negative regulator of transcription. The second observation is that there are a number of genes that were up-regulated in response to

MEF2A knockdown in MBs including *Tprg*, *Mctp2*, *Kitl*, *Prrx1* and *Dusp6*. Repression of these genes may not be solely regulated by MEF2 as AP-1 binding sites, which are associated with proliferation, are frequently found not only in MEF2 enriched binding sites (as reported here in both CM and MB) but also in MyoD target genes (46). AP-1 and MyoD are known to antagonize each other's function through direct protein–protein interactions (68,69), and yet together, can also form MyoD-directed enhancers (70). Based on data presented here it is likely that MEF2 may either have a role in AP-1-MyoD-dependent gene expression, or AP-1 and MEF2 may function in combination and independently of MyoD to regulate developmental processes.

Using high-throughput genomic approaches we have identified a comprehensive list of MEF2 target genes in skeletal and cardiac muscle that will be further investigated in a variety of cellular contexts. Mechanistic smaller scale follow-up studies based on the high-throughput data have so far revealed the novel observation that MEF2 represses *Dusp6* in skeletal and cardiac muscle and this is p38MAPK-dependent in MBs. Understanding the global role of MEF2 in striated muscle gene expression has implications not only for our understanding of development, but also in contexts where the expression of developmental genes is recapitulated, such as in post-natal skeletal muscle regeneration and cardiac hypertrophy.

ACCESSION NUMBERS

Gene Expression Omnibus (GEO) accession number: GSE61207

SUPPLEMENTARY DATA

Supplementary Data are available at NAR Online.

ACKNOWLEDGEMENT

The authors would like to thank Stephen M. Keyse (Ninewells Hospital and Medical School, Dundee, UK) for the *Dusp6*-luciferase construct.

FUNDING

Canadian Institutes of Health Research [102688 to J.C.M., 120349 to A.B.]. Funding for open access charge: Canadian Institutes of Health Research (CIHR).
Conflict of interest statement. None declared.

REFERENCES

1. Lin,Q., Lu,J., Yanagisawa,H., Webb,R., Lyons,G.E., Richardson,J.A. and Olson,E.N. (1998) Requirement of the MADS-box transcription factor MEF2C for vascular development. *Development*, **125**, 4565–4574.
2. Edmondson,D.G., Lyons,G.E., Martin,J.F. and Olson,E.N. (1994) Mef2 gene-expression marks the cardiac and skeletal-muscle lineages during mouse embryogenesis. *Development*, **120**, 1251–1263.
3. Lyons,G.E., Micales,B.K., Schwarz,J., Martin,J.F. and Olson,E.N. (1995) Expression of Mef2 genes in the mouse central-nervous-system suggests a role in neuronal maturation. *J. Neurosci.*, **15**, 5727–5738.
4. Woronicz,J.D., Lina,A., Calnan,B.J., Szychowski,S., Cheng,L. and Winoto,A. (1995) Regulation of the Nur77 orphan steroid-receptor in activation-induced apoptosis. *Mol. Cell. Biol.*, **15**, 6364–6376.
5. Pollock,R. and Treisman,R. (1991) Human srf-related proteins—dna-binding properties and potential regulatory targets. *Genes Dev.*, **5**, 2327–2341.
6. Andres,V., Cervera,M. and Mahdavi,V. (1995) Determination of the consensus binding-site for Mef2 expressed in muscle and brain reveals tissue-specific sequence constraints. *J. Biol. Chem.*, **270**, 23246–23249.
7. Han,J., Jiang,Y., Li,Z., Kravchenko,V. and Ulevitch,R. (1997) Activation of the transcription factor MEF2C by the MAP kinase p38 in inflammation. *Nature*, **386**, 296–299.
8. Zetser,A., Gredinger,E. and Bengal,E. (1999) p38 mitogen-activated protein kinase pathway promotes skeletal muscle differentiation—participation of the MEF2C transcription factor. *J. Biol. Chem.*, **274**, 5193–5200.
9. Kato,Y., Kravchenko,V., Tapping,R., Han,J., Ulevitch,R. and Lee,J. (1997) BMK1/ERK5 regulates serum-induced early gene expression through transcription factor MEF2C. *EMBO J.*, **16**, 7054–7066.
10. Du,M., Perry,R.L.S., Nowacki,N.B., Gordon,J.W., Salma,J., Zhao,J., Aziz,A., Chan,J., Siu,K.W.M. and McDermott,J.C. (2008) Protein kinase a represses skeletal myogenesis by targeting myocyte enhancer factor 2D. *Mol. Cell. Biol.*, **28**, 2952–2970.
11. Miska,E.A., Karlsson,C., Langley,E., Nielsen,S.J., Pines,J. and Kouzarides,T. (1999) HDAC4 deacetylase associates with and represses the MEF2 transcription factor. *EMBO J.*, **18**, 5099–5107.
12. Lu,J.R., McKinsey,T.A., Zhang,C.L. and Olson,E.N. (2000) Regulation of skeletal myogenesis by association of the MEF2 transcription factor with class II histone deacetylases. *Mol. Cell*, **6**, 233–244.
13. Lin,Q., Schwarz,J., Bucana,C. and Olson,E.N. (1997) Control of mouse cardiac morphogenesis and myogenesis by transcription factor MEF2C. *Science*, **276**, 1404–1407.
14. Naya,F.J., Wu,C.Z., Richardson,J.A., Overbeek,P. and Olson,E.N. (1999) Transcriptional activity of MEF2 during mouse embryogenesis monitored with a MEF2-dependent transgene. *Development*, **126**, 2045–2052.
15. Zhang,C.L., McKinsey,T.A., Chang,S.R., Antos,C.L., Hill,J.A. and Olson,E.N. (2002) Class II histone deacetylases act as signal-responsive repressors of cardiac hypertrophy. *Cell*, **110**, 479–488.
16. Liu,N., Nelson,B.R., Bezprozvannaya,S., Shelton,J.M., Richardson,J.A., Bassel-Duby,R. and Olson,E.N. (2014) Requirement of MEF2A, C, and D for skeletal muscle regeneration. *Proc. Natl. Acad. Sci. U.S.A.*, **111**, 4109–4114.
17. Naya,F., Black,B., Wu,H., Bassel-Duby,R., Richardson,J., Hill,J. and Olson,E. (2002) Mitochondrial deficiency and cardiac sudden death in mice lacking the MEF2A transcription factor. *Nat. Med.*, **8**, 1303–1309.
18. Kim,Y., Phan,D., Van Rooij,E., Wang,D., McAnally,J., Qi,X., Richardson,J.A., Hill,J.A., Bassel-Duby,R. and Olson,E.N. (2008) The MEF2D transcription factor mediates stress-dependent cardiac remodeling in mice. *J. Clin. Invest.*, **118**, 124–132.
19. Potthoff,M.J., Wu,H., Arnold,M.A., Shelton,J.M., Backs,J., McAnally,J., Richardson,J.A., Bassel-Duby,R. and Olson,E.N. (2007) Histone deacetylase degradation and MEF2 activation promote the formation of slow-twitch myofibers. *J. Clin. Invest.*, **117**, 2459–2467.
20. Potthoff,M.J., Arnold,M.A., McAnally,J., Richardson,J.A., Bassel-Duby,R. and Olson,E.N. (2007) Regulation of skeletal muscle sarcomere integrity and postnatal muscle function by Mef2c. *Mol. Cell. Biol.*, **27**, 8143–8151.
21. Passier,R., Zeng,H., Frey,N., Naya,F.J., Nicol,R.L., McKinsey,T.A., Overbeek,P., Richardson,J.A., Grant,S.R. and Olson,E.N. (2000) CaM kinase signaling induces cardiac hypertrophy and activates the MEF2 transcription factor in vivo. *J. Clin. Invest.*, **105**, 1395–1406.
22. Vega,R., Harrison,B., Meadows,E., Roberts,C., Papst,P., Olson,E. and McKinsey,T. (2004) Protein kinases C and D mediate agonist-dependent cardiac hypertrophy through nuclear export of histone deacetylase 5. *Mol. Cell. Biol.*, **24**, 8374–8385.
23. Sartorelli,V., Kurabayashi,M. and Kedes,L. (1993) Muscle-specific gene-expression—a comparison of cardiac and skeletal-muscle transcription strategies. *Circ. Res.*, **72**, 925–931.

24. Blais,A., Tsikitis,M., Acosta-Alvear,D., Sharan,R., Kluger,Y. and Dynlacht,B.D. (2005) An initial blueprint for myogenic differentiation. *Genes Dev.*, **19**, 553–569.
25. Schlesinger,J., Schueler,M., Grunert,M., Fischer,J.J., Zhang,Q., Krueger,T., Lange,M., Toenjes,M., Dunkel,I. and Sperling,S.R. (2011) The cardiac transcription network modulated by Gata4, Mef2a, Nkx2.5, srf, histone modifications, and MicroRNAs. *PloS Genet.*, **7**, e1001313.
26. Sebastian,S., Faralli,H., Yao,Z., Rakopoulos,P., Palii,C., Cao,Y., Singh,K., Liu,Q., Chu,A., Aziz,A. *et al.* (2013) Tissue-specific splicing of a ubiquitously expressed transcription factor is essential for muscle differentiation. *Genes Dev.*, **27**, 1247–1259.
27. Youn,H.D., Sun,L., Prywes,R. and Liu,J.O. (1999) Apoptosis of T cells mediated by Ca2+-induced release of the transcription factor MEF2. *Science*, **286**, 790–793.
28. Mao,Z.X., Bonni,A., Xia,F., Nadal-Vicens,M. and Greenberg,M.E. (1999) Neuronal activity-dependent cell survival mediated by transcription factor MEF2. *Science*, **286**, 785–790.
29. Wilker,P.R., Kohyama,M., Sandau,M.M., Albring,J.C., Nakagawa,O., Schwarz,J.J. and Murphy,K.M. (2008) Transcription factor Mef2c is required for B cell proliferation and survival after antigen receptor stimulation. *Nat. Immunol.*, **9**, 603–612.
30. Salma,J. and McDermott,J.C. (2012) Suppression of a MEF2-KLF6 survival pathway by PKA signaling promotes apoptosis in embryonic hippocampal neurons. *J. Neurosci.*, **32**, 2790–2803.
31. Rhee,H.S. and Pugh,B.F. (2011) Comprehensive genome-wide protein-DNA interactions detected at single-nucleotide resolution. *Cell*, **147**, 1408–1419.
32. Ornatsky,O.I., Cox,D.M., Tangirala,P., Andreucci,J.J., Quinn,Z.A., Wrana,J.L., Prywes,R., Yu,Y.T. and McDermott,J.C. (1999) Post-translational control of the MEF2A transcriptional regulatory protein. *Nucleic Acids Res.*, **27**, 2646–2654.
33. Ekerot,M., Stavridis,M.P., Delavaine,L., Mitchell,M.P., Staples,C., Owens,D.M., Keenan,I.D., Dickinson,R.J., Storey,K.G. and Keyse,S.M. (2008) Negative-feedback regulation of FGF signalling by DUSP6/MKP-3 is driven by ERK1/2 and mediated by ets factor binding to a conserved site within the DUSP6/MKP-3 gene promoter. *Biochem. J.*, **412**, 287–298.
34. Cox,D.M., Du,M., Marback,M., Yang,E.C.C., Chan,J., Siu,K.W.M. and McDermott,J.C. (2003) Phosphorylation motifs regulating the stability and function of myocyte enhancer factor 2A. *J. Biol. Chem.*, **278**, 15297–15303.
35. Dionyssiou,M.G., Salma,J., Bevzyuk,M., Wales,S., Zakharyan,L. and McDermott,J.C. (2013) Kruppel-like factor 6 (KLF6) promotes cell proliferation in skeletal myoblasts in response to TGFbeta/Smad3 signaling. *Skelet. Muscle*, **3**, 7.
36. Li,H. and Durbin,R. (2009) Fast and accurate short read alignment with Burrows-Wheeler transform. *Bioinformatics*, **25**, 1754–1760.
37. Li,H., Handsaker,B., Wysoker,A., Fennell,T., Ruan,J., Homer,N., Marth,G., Abecasis,G., Durbin,R. and 1000 Genome Project Data Processing Subgroup (2009) The Sequence Alignment/Map format and SAMtools. *Bioinformatics*, **25**, 2078–2079.
38. Zhang,Y., Liu,T., Meyer,C.A., Eeckhoute,J., Johnson,D.S., Bernstein,B.E., Nussbaum,C., Myers,R.M., Brown,M., Li,W. *et al.* (2008) Model-based analysis of ChIP-seq (MACS). *Genome Biol.*, **9**, R137.
39. Kent,W.J., Sugnet,C.W., Furey,T.S., Roskin,K.M., Pringle,T.H., Zahler,A.M. and Haussler,D. (2002) The human genome browser at UCSC. *Genome Res.*, **12**, 996–1006.
40. Bolger,A.M., Lohse,M. and Usadel,B. (2014) Trimmomatic: a flexible trimmer for Illumina sequence data. *Bioinformatics*, **30**, 2114–2120.
41. Trapnell,C., Pachter,L. and Salzberg,S.L. (2009) TopHat: discovering splice junctions with RNA-Seq. *Bioinformatics*, **25**, 1105–1111.
42. Robinson,M.D., McCarthy,D.J. and Smyth,G.K. (2010) edgeR: a Bioconductor package for differential expression analysis of digital gene expression data. *Bioinformatics*, **26**, 139–140.
43. Anders,S. and Huber,W. (2010) Differential expression analysis for sequence count data. *Genome biol.*, **11**, R106.
44. McLean,C.Y., Bristor,D., Hiller,M., Clarke,S.L., Schaar,B.T., Lowe,C.B., Wenger,A.M. and Bejerano,G. (2010) GREAT improves functional interpretation of cis-regulatory regions. *Nat. Biotechnol.*, **28**, 495–501.
45. Zhang,Z., Chang,C.W., Goh,W.L., Sung,W. and Cheung,E. (2011) CENTDIST: discovery of co-associated factors by motif distribution. *Nucleic Acids Res.*, **39**, W391–W399.
46. Cao,Y., Yao,Z., Sarkar,D., Lawrence,M., Sanchez,G.J., Parker,M.H., MacQuarrie,K.L., Davison,J., Morgan,M.T., Ruzzo,W.L. *et al.* (2010) Genome-wide MyoD binding in skeletal muscle cells: a potential for broad cellular reprogramming. *Dev. Cell*, **18**, 662–674.
47. Boyle,E.I., Weng,S.A., Gollub,J., Jin,H., Botstein,D., Cherry,J.M. and Sherlock,G. (2004) GO::TermFinder—open source software for accessing gene ontology information and finding significantly enriched gene ontology terms associated with a list of genes. *Bioinformatics*, **20**, 3710–3715.
48. Robinson,J.T., Thorvaldsdottir,H., Winckler,W., Guttman,M., Lander,E.S., Getz,G. and Mesirov,J.P. (2011) Integrative genomics viewer. *Nat. Biotechnol.*, **29**, 24–26.
49. Maillet,M., Purcell,N.H., Sargent,M.A., York,A.J., Bueno,O.F. and Molkentin,J.D. (2008) DUSP6 (MKP3) null mice show enhanced ERK1/2 phosphorylation at baseline and increased myocyte proliferation in the heart affecting disease susceptibility. *J. Biol. Chem.*, **283**, 31246–31255.
50. Le Grand,F., Grifone,R., Mourikis,P., Houbron,C., Gigaud,C., Pujol,J., Maillet,M., Pages,G., Rudnicki,M., Tajbakhsh,S. *et al.* (2012) Six1 regulates stem cell repair potential and self-renewal during skeletal muscle regeneration. *J. Cell Biol.*, **198**, 815–832.
51. Ornatsky,O.I. and McDermott,J.C. (1996) MEF2 protein expression, DNA binding specificity and complex composition, and transcriptional activity in muscle and non-muscle cells. *J. Biol. Chem.*, **271**, 24927–24933.
52. Groom,L.A., Sneddon,A.A., Alessi,D.R., Dowd,S. and Keyse,S.M. (1996) Differential regulation of the MAP, SAP and RK/p38 kinases by Pyst1, a novel cytosolic dual-specificity phosphatase. *EMBO J.*, **15**, 3621–3632.
53. Muda,M., Theodosiou,A., Rodrigues,N., Boschert,U., Camps,M., Gillieron,C., Davies,K., Ashworth,A. and Arkinstall,S. (1996) The dual specificity phosphatases M3/6 and MKP-3 are highly selective for inactivation of distinct mitogen-activated protein kinases. *J. Biol. Chem.*, **271**, 27205–27208.
54. Li,C., Scott,D.A., Hatch,E., Tian,X. and Mansour,S.L. (2007) Dusp6 (Mkp3) is a negative feedback regulator of FGF-stimulated ERK signaling during mouse development. *Development*, **134**, 167–176.
55. Ornatsky,O.I., Andreucci,J.J. and McDermott,J.C. (1997) A dominant-negative form of transcription factor MEF2 inhibits myogenesis. *J. Biol. Chem.*, **272**, 33271–33278.
56. Yang,S., Kalkan,T., Morrisroe,C., Smith,A. and Sharrocks,A.D. (2012) A genome-wide RNAi screen reveals MAP kinase phosphatases as key ERK pathway regulators during embryonic stem cell differentiation. *PLoS Genet.*, **8**, e1003112.
57. Auger-Messier,M., Accornero,F., Goonasekera,S.A., Bueno,O.F., Lorenz,J.N., van Berlo,J.H., Willette,R.N. and Molkentin,J.D. (2012) Unrestrained p38 MAPK activation in Dusp1/4 double-null mice induces cardiomyopathy. *Circ. Res.*, **112**, 48–56.
58. Wu,Z., Woodring,P., Bhakta,K., Tamura,K., Wen,F., Feramisco,J., Karin,M., Wang,J. and Puri,P. (2000) P38 and extracellular signal-regulated kinases regulate the myogenic program at multiple steps. *Mol. Cell. Biol.*, **20**, 3951–3964.
59. Bennett,A.M. and Tonks,N.K. (1997) Regulation of distinct stages of skeletal muscle differentiation by mitogen-activated protein kinases. *Science*, **278**, 1288–1291.
60. Li,J. and Johnson,S.E. (2006) ERK2 is required for efficient terminal differentiation of skeletal myoblasts. *Biochem. Biophys. Res. Commun.*, **345**, 1425–1433.
61. Youn,H.D. and Liu,J.O. (2000) Cabin1 represses MEF2-dependent Nur77 expression and T cell apoptosis by controlling association of histone deacetylases and acetylases with MEF2. *Immunity*, **13**, 85–94.
62. Sparrow,D.B., Miska,E.A., Langley,E., Reynaud-Deonauth,S., Kotecha,S., Towers,N., Spohr,G., Kouzarides,T. and Mohun,T.J. (1999) MEF-2 function is modified by a novel co-repressor, MITR. *EMBO J.*, **18**, 5085–5098.
63. de la Vega,L., Hornung,J., Kremmer,E., Milanovic,M. and Schmitz,M.L. (2013) Homeodomain-interacting protein kinase 2-dependent repression of myogenic differentiation is relieved by its caspase-mediated cleavage. *Nucleic Acids Res.*, **41**, 5731–5745.
64. Gordon,J.W., Pagiatakis,C., Salma,J., Du,M., Andreucci,J.J., Zhao,J., Hou,G., Perry,R.L., Dan,Q., Courtman,D. *et al.* (2009) Protein

kinase A-regulated assembly of a MEF2.HDAC4 repressor complex controls c-jun expression in vascular smooth muscle cells. *J. Biol. Chem.*, **284**, 19027–19042.
65. Weston,A.D., Sampaio,A.V., Ridgeway,A.G. and Underhill,T.M. (2003) Inhibition of p38 MAPK signaling promotes late stages of myogenesis. *J. Cell. Sci.*, **116**, 2885–2893.
66. Sandmann,T., Jensen,L.J., Jakobsen,J.S., Karzynski,M.M., Eichenlaub,M.P., Bork,P. and Furlong,E.E.M. (2006) A temporal map of transcription factor activity: Mef2 directly regulates at all stages of muscle target genes development. *Dev. Cell*, **10**, 797–807.
67. Papait,R., Cattaneo,P., Kunderfranco,P., Greco,C., Carullo,P., Guffanti,A., Vigano,V., Stirparo,G.G., Latronico,M.V.G., Hasenfuss,G. *et al.* (2013) Genome-wide analysis of histone marks identifying an epigenetic signature of promoters and enhancers underlying cardiac hypertrophy. *Proc. Natl. Acad. Sci. U.S.A.*, **110**, 20164–20169.
68. Bengal,E., Ransone,L., Scharfmann,R., Dwarki,V.J., Tapscott,S.J., Weintraub,H. and Verma,I.M. (1992) Functional antagonism between C-jun and myod proteins—a direct physical association. *Cell*, **68**, 507–519.
69. Li,L., Chambard,J.C., Karin,M. and Olson,E.N. (1992) Fos and jun repress transcriptional activation by myogenin and myod—the amino terminus of jun can mediate repression. *Genes Dev.*, **6**, 676–689.
70. Blum,R., Vethantham,V., Bowman,C., Rudnicki,M. and Dynlacht,B.D. (2012) Genome-wide identification of enhancers in skeletal muscle: the role of MyoD1. *Genes Dev.*, **26**, 2763–2779.